Published in final edited form as:
Neuroimage. 2010 October 1; 52(4): 1420–1427. doi:10.1016/j.neuroimage.2010.05.014.

BOLD fMRI of visual and somatosensory–motor stimulations in baboons

Hsiao-Ying Wey[a,b], **Jinqi Li**[a], **C. Ákos Szabó**[c], **Peter T. Fox**[a,b,c,e], **M. Michelle Leland**[f], **Lisa Jones**[f], and **Timothy Q. Duong**[a,b,d,e,*]

[a]Research Imaging Institute, University of Texas Health Science Center, San Antonio, TX, USA

[b]Department of Radiology, University of Texas Health Science Center, San Antonio, TX, USA

[c]Department of Neurology, University of Texas Health Science Center, San Antonio, TX, USA

[d]Department of Ophthalmology, University of Texas Health Science Center, San Antonio, TX, USA

[e]Department of Physiology, University of Texas Health Science Center, San Antonio, TX, USA

[f]Laboratory Animal Resources, University of Texas Health Science Center, San Antonio, TX, USA

Abstract

Baboon, with its large brain size and extensive cortical folding compared to other non-human primates, serves as a good model for neuroscience research. This study reports the implementation of a baboon model for blood oxygenation level-dependent (BOLD) fMRI studies (1.5 × 1.5 × 4 mm resolution) on a clinical 3 T-MRI scanner. BOLD fMRI responses to hypercapnic (5% CO_2) challenge, 10 Hz flicker visual, and vibrotactile somatosensory–motor stimulations were investigated in baboons anesthetized sequentially with isoflurane and ketamine. Hypercapnia evoked robust BOLD increases. Paralysis was determined to be necessary to achieve reproducible functional activations within and between subjects under our experimental conditions. With optimized anesthetic doses (0.8–1.0% isoflurane or 6–8 mg/kg/h ketamine) and adequate paralysis (vecuronium, 0.2 mg/kg), robust activations were detected in the visual (V), primary (S1) and secondary (S2) somatosensory, primary motor (M cortices), supplementary motor area (SMA), lateral geniculate nucleus (LGN) and thalamus (Th). Data were tabulated for 11 trials under isoflurane and 10 trials under ketamine on 5 baboons. S1, S2, M, and V activations were detected in essentially all trials (90–100% of the time, except 82% for S2 under isoflurane and 70% for M under ketamine). LGN activations were detected 64–70% of the time under both anesthetics. SMA and Th activations were detected 36–45% of the time under isoflurane and 60% of the time under ketamine. BOLD percent changes among different structures were slightly higher under ketamine than isoflurane (0.75% versus 0.58% averaging all structures), but none was statistically different ($P>0.05$). This baboon model offers an opportunity to non-invasively image brain functions and dysfunctions in large non-human primates.

Keywords

Blood oxygenation level-dependent (BOLD); fMRI; Non-human primates; Cerebral blood flow; Thalamus; Brain mapping; Anesthetic; Animal models

*Corresponding author. Research Imaging Institute, UTHSCSA, 8403 Floyd Curl Drive, San Antonio, TX 78229, USA. Fax: +1 210 567 8152. duongt@uthscsa.edu (T.Q. Duong).

Introduction

Non-human primates (NHPs) are important animal models because of their similarities to humans, resulting in better recapitulation of human diseases compared to rodents (Fisher, 1999; Fukuda and del Zoppo, 2003; Killam, 1979; Rogers and Hixson, 1997). In particular, baboons (*Papio hamadryas species*) are Old World monkeys who are evolutionary the closest to human besides Great Apes. A unique characteristic of the baboons is that they have large brain volume (i.e., more than twice that of macaques) with extensive cortical folding (Kochunov and Davis, 2009; Leigh, 2004), making them more amenable to imaging studies using magnetic resonance imaging (MRI) and positron emission tomography (PET). In addition, baboons, in contrast to macaques, do not carry the herpes B virus, which could be fatal to humans if infected. As such, baboons have been widely used in research studies of stroke (Del Zoppo et al., 1986; Fukuda and del Zoppo, 2003), epilepsy (Fisher, 1989; Szabó et al., 2007), infection diseases and vaccine development (Kennedy et al., 1997; Locher et al., 2001), among others, providing more clinically relevant models of human diseases.

Blood oxygenation level-dependent (BOLD) functional magnetic resonance imaging (fMRI) has become a powerful imaging tool for mapping brain functions non-invasively. fMRI of restrained and awake rhesus (Andersen et al., 2002; Dubowitz et al., 2001a,b; Gamlin et al., 2006; Logothetis et al., 1999; Pinsk et al., 2005; Vanduffel et al., 2001) and marmoset (Ferris et al., 2001, 2004) have found many important neuroscience applications. fMRI studies of awake NHPs necessitate acclimation to restraining devices to minimize stress and reduce motion artifacts (King et al., 2005; Stefanacci et al., 1998). No fMRI study of awake baboon has been reported to our knowledge, likely because restraining baboons are considerably more challenging simply due to their sizes. In contrast to awake NHP studies, fMRI of anesthetized NHPs are sparse (Chen et al., 2007; Logothetis, 2002; Wibral et al., 2007). While anesthetics minimize stress and motion artifacts, they suppress neuronal response to stimulations and may have systemic cerebrovascular effects (e.g., isoflurane is a known vasodilator) (Logothetis et al., 1999; Sicard et al., 2003). Type of anesthetic and dosage thus need to be carefully considered. Paralytic may be needed to eliminate motion, allowing minimal anesthetic dose. Although anesthetized NHP models preclude fMRI studies of higher order cognitive functions, fMRI of primary sensory systems in anesthetized NHPs offers an invaluable tool for neuroscience research, including investigation of normal cerebral physiology and patho-physiology of neurological diseases.

Custom-designed MRI scanners for large NHP fMRI have been utilized but their availability is limited (Gamlin et al., 2006; Logothetis et al., 1999). As such, large NHP fMRI studies are widely performed on clinical scanners. A major challenge in NHP fMRI on clinical scanner is achieving adequate spatial resolution given their smaller brain size, such that comparable parcellation of functional structures to the human brain can be achieved (Stelkis and Erwin, 1988; Stephan et al., 1981). Although the typical clinical magnetic field gradients and radiofrequency coils are suboptimal for NHPs, fMRI studies on human scanner remain popular because of the ease of use and translation (Duong, 2010).

This study reports the implementation of an anesthetized baboon model for BOLD fMRI studies on a clinical 3 Tesla scanner with the long-term goals of applying this model to stroke and epilepsy research. BOLD fMRI responses to hypercapnic challenge, visual and somatosensory–motor stimulations were investigated in baboons anesthetized sequentially with two commonly used anesthetics (isoflurane and ketamine). BOLD fMRI studies were also compared with and without a common paralytic (vecuronium). Optimization of the animal model for fMRI studies, challenges encountered and solutions are described. To our knowledge, this is the first report of BOLD fMRI study on baboons.

Methods

Animal preparations

Normal female baboons (*Papio hamadryas species*, 10–20 kg, 16 ± 4 kg, $n = 7$) were studied with approval from the Institutional Animal Care and Use Committee of the University of Texas Health Science Center at San Antonio. Each animal was initially inducted using ketamine (1.0–1.2 mg, i.m.) for oral intubation and catheterization of a venous line (saphenous vein) and was maintained with 1.5–2.0% isoflurane in air in preparation for MRI. Animals were mechanically ventilated using a mechanical ventilator (Aestiva 5 from Datex-Ohmeda, Madison, WI) at 8–12 stroke/min, 120–180 ml/stroke, ~8 cm of water pressure. Animal was positioned supine, stabilized in a custom-made animal holder with ear bars, mouth bar and padding around the head. Both eyelids were kept open for visual stimulation and eye ointment was applied to prevent corneal dryness. Body temperature was maintained by using a custom-built feedback-regulated circulating warm-air blanket. End-tidal CO_2 ($ETCO_2$), O_2 saturation, heart rate, respiration rate, and rectal temperature were monitored continuously using an MRI-compatible physiological monitoring equipment (Precess from Invivo, Orlando, FL). In two animals, femoral artery was catheterized percutaneously for blood–gas sampling to correlate with $ETCO_2$ values, which were not accurate due to the long sampling line but was precise and non-invasive for gauging blood pCO_2.

fMRI studies were performed first under 0.8–1.0% isoflurane, taking about 2 h. The anesthetic was then switched to intravenous ketamine (6–8 mg/kg/h, administered *via* a MRI-compatible injector, Continuum MR Compatible Infusion System, MEDRAD, New York, NY) and isoflurane was discontinued 15 min after ketamine onset. To avoid confounds of mixing anesthetics on BOLD signals, fMRI acquisitions started 20–30 min after isoflurane was switched off and continued for an additional 2 h under ketamine. In the initial studies (Group I: 2 sessions, 2 baboons), experiments were performed without paralytics. In subsequent studies (Group II: 10 sessions on 5 baboons) experiments were performed with a paralytic (vecuronium 0.2 mg/kg initial dose, followed by 10% of initial dose every 45–90 min). The first dose of vecuronium was administered immediately before placing the animal into the center of MRI scanner. At the end of the fMRI experiments, neostigmine (0.5–2 mg, i.v.) with atropine (0.6–1.2 mg, i.v.) was administered to reverse paralysis.

Stimulations

Hypercapnic challenge utilized a paradigm of 2 min air, 2 min 5% CO_2 in air a pre-mixed tank). Hypercapnia was applied once under each anesthetic. A 10–15 min break was given after stimulation to eliminate the effects of hypercapnia. Binocular visual stimulation used achromatic light flickering at 10 Hz was delivered *via* two fiber-optic cables placed in front of the eyes. Somatosensory–motor stimulation was applied to the animal's right hand *via* a custom-made pneumatic-driven vibrotactile stimulator. The hand was secured around the stimulator. Both visual and somatosensory–motor stimulations were applied simultaneously to induce large number of activated pixels in different brain areas at the same time, while minimizing the anesthesia duration. An fMRI stimulation block consisted of three epochs of (50 s OFF and 50 s ON), followed by 50 s OFF. Typically, 1–3 fMRI stimulation trials were repeated in each session for each anesthetic.

MRI

All MRI studies were performed on a Siemens TIM-Trio 3 T clinical scanner with a body radiofrequency (RF) coil for transmission and a standard 12-channel head RF coil for reception (Siemens, Erlangen, Germany). BOLD fMRI was acquired using gradient-echo, echo-planar imaging (EPI), TR=2.5 s, TE=30 ms, matrix=100 × 100 or 64 × 64, field of view (FOV) = 150 × 150 or 128 × 128 mm, and 12 or 10 contiguous axial slices (respectively) covering essentially

the entire cerebrum. The corresponding spatial resolutions were 1.5 × 1.5 × 4 or 2 × 2 × 5 mm. For hypercapnic challenge, a time series of 144 images were acquired, with a total scan time of 6 min. For functional stimulation, three epochs of (20 images OFF and 20 images ON) were acquired followed by 20 images OFF, with a total scan time of 5 min 48 s.

High-resolution anatomical images were also acquired using the MP-RAGE sequence with following parameters: TR/TE/flip angle = 2100 ms/3.1 ms/12°, non-selective inversion pulse, TI = 1100 ms, FOV = 16 × 19.2 × 19.2 cm, 1 mm isotropic spatial resolution. Anatomical images were typically acquired during the transition between the two anesthetics.

Data analysis

fMRI data were processed using FMRIB Software Library (FSL) (Smith et al., 2004; Woolrich et al., 2009) and codes written in MATLAB (Math Works, Natick, MA). Image pre-processing included skull stripping, motion correction, temporal filtering, and spatial smoothing with a Gaussian filter of 5 mm at FWHM. A non-linear Gaussian temporal filter was applied using a high-pass threshold of 100 s and a low-pass threshold of 1.6–2.5 s (depending on the ventilated respiration rates) (Bianciardi et al., 2004; Smith et al., 2005). Activation maps were generated using the general linear modeling (GLM) in the FEAT toolbox in FSL on a voxel-by-voxel basis and a threshold of $Z > 2.3$ ($p < 0.01$). All echo-planar images were co-registered first to their own anatomical images and then to a high-resolution template (0.4 mm isotropic resolution) from a population-based, pseudo-Talairach, median-geometry atlas (Kochunov and Davis, 2009).

Hypercapnic-induced BOLD percent signal changes of the whole-brain were calculated and statistically analyzed between the two anesthetics using paired t-tests ($p < 0.05$). Region-of-interest (ROI) analysis was performed on the primary (S1) and secondary (S2) somatosensory cortex, primary motor cortex (M), supplementary motor area (SMA), thalamus (Th), visual cortex (V), and lateral geniculate nuclei (LGN). ROIs were chosen manually with reference to the baboon MRI atlas (Greer et al., 2002). Within a single scan, three epochs were averaged into a single epoch with the first five time points (non-steady state) discarded. A total of eleven trials under isoflurane and 10 trials under ketamine from 5 baboons (with paralytic) were analyzed in detail. Averaged time courses from all trials were plotted with mean ± SEM. BOLD percent changes were tabulated as mean ± SEM. Paired t-tests between the two anesthetics were analyzed with $p < 0.05$ taken to be statistically significant.

Results

Physiology

All measured physiological parameters were maintained within normal physiological ranges. Under isoflurane and ketamine, respectively, the heart rates were 101 ± 42 and 119 ± 19 bpm; respiration rates 11.7 ± 1.0 and 11.4 ± 0.9 bpm; tidal volumes 169 ± 38 and 169 ± 38 ml; $ETCO_2$ values 36 ± 5 and 36 ± 4 mmHg; and rectal temperatures 99 ± 2 °F and 99 ± 2 °F; (mean±SD, 10 sessions, 5 animals). None of the measured parameter was statistically different between the two anesthetics. These physiological parameters were also not statistically different between with and without paralytics (data without paralytics are not shown).

Blood–gas measurements (4 samples from 2 animals) were made to confirm normal physiological parameters under isoflurane with paralytic. The measured blood–gas parameters were: pO_2 = 105 ± 4 mmHg, pCO_2=37 ± 8 mmHg, and pH = 7.47 ± 0.04. The corresponding oxygen saturation and $ETCO_2$ made at the time of the blood–gas measurements were 98 ± 0% and 33.0 ± 3.5 mmHg, respectively. Note that $ETCO_2$ is known to be slightly lower (~5 mmHg) than arterial pCO_2 (Jones et al., 1979; Takano et al., 2003).

Effects of anesthetics on BOLD fMRI

At 1.2–1.5% isoflurane, BOLD responses to visual and vibrotactile stimulations were seldom detected. Hypercapnia under 1.2–1.5% isoflurane was not studied, although a hypercapnia-induced BOLD response should be detectable but the percent changes were smaller compared to that at lower isoflurane level, consistent with a previous rat study (Sicard et al., 2003). In Group I, with 0.8–1.0% isoflurane without paralytic, the animals remained adequately anesthetized as determined by the absence of pinching responses (such as physical responses or increased heart rate). Hypercapnic challenge was reliably detected without paralytic. Activations by visual and somatosensory–motor stimuli were often detected in the expected brain regions. Although gross motion was rare, BOLD fMRI data were often contaminated by signal drifts and large temporal fluctuations, likely due to minor motion and physiological noises (data not shown). fMRI data qualities were inconsistent in repeated fMRI trials within the same sessions as well as between sessions. Similar findings were reported with ketamine at a minimal dose (6–8 mg/kg/h) that adequately anesthetized the animals without paralytics.

By contrast, with vecuronium paralysis (Group II), the BOLD fMRI time courses were stable, and BOLD activations were robust and consistent across multiple repeated fMRI trials in the same sessions and between animals for both isoflurane and ketamine anesthesia. Paralysis was effectively reversed by neostigmine. All animals were able to breathe unassisted within 5–10 min and became fully conscious typically within 10–20 min after administration of neostigmine. All subsequent studies thus utilized vecuronium for paralysis.

Note that about half an hour was given when switching between the two anesthetics before fMRI measurements under ketamine in order to minimize possible confounding effects of mixing anesthetics. This timing was chosen based on separation observations that it took only 5– 10 min for the baboon without paralytic to become conscious and responsive after isoflurane was discontinued. However, there could be some potential residue effects of isoflurane; this was however not investigated in the present study.

BOLD fMRI

Hypercapnia, known to increase cerebral blood flow, was observed to increase BOLD signal. Whole-brain BOLD increases were reliably detected. Fig. 1A shows the BOLD map from a representative subject under isoflurane. The group-averaged time courses during hypercapnic challenge under isoflurane and ketamine with paralytic (Group II) are shown in Fig. 1B. Hypercapnia-induced BOLD percent change of the whole-brain was 1.19±0.40% under isoflurane and 1.24±0.38% under ketamine (mean ± SEM, 3 trials for each anesthetic; 3 sessions on 2 baboons). No statistical difference was found in BOLD signal changes between the two anesthetics ($p > 0.05$).

Simultaneous binocular visual and unilateral somatosensory– motor stimulations activate V, S1, S2, M, SMA, Th, and LGN under both anesthetics. Fig. 2 shows activation maps of a single subject under isoflurane and ketamine both with paralytic (Group II). Robust and reproducible functional activations were detected in the primary cortices. Moreover, activations were often detected in the subcortical regions such as the Th and LGN. Binocular visual stimulation activated both hemispheres of V and LGN. Unilateral stimulation to the hand activated the contralateral S1 and contralateral M (the ROI likely included premotor cortex). Interestingly, bilateral activations of the S2, Th and SMA were detected.

To demonstrate reproducibility across trials, Fig. 3 shows all individual fMRI traces from the S1 ROI for the two anesthetics. The stimulus-evoked percent changes ranged from 0.3% to 0.89% under isoflurane and 0.42% to 1.0% under ketamine. Fig. 4 shows the group-averaged BOLD time courses for the above-described structures obtained from the ROIs depicted in Fig.

2C. Both isoflurane and ketamine yielded reliable fMRI responses. Percent changes were similar between isoflurane and ketamine, suggesting comparable BOLD fMRI sensitivity.

Group-averaged BOLD percent changes and frequencies of detectable activation are summarized in Table 1. BOLD percent changes were not statistically different between the two anesthetics ($P>0.05$). The averaged Z scores – ranging from 4.0 to 5.5 – were also not statistically different between the two anesthetics ($P>0.05$). S1, S2, V and M activations were detected essentially in all trials and all studies (90–100% of the time, except 82% for S2 under isoflurane and 70% for M under ketamine). LGN activations were detected 64–70% of the time for both anesthetics. SMA and Th activations were detected 36–45% of the time under isoflurane and 60% of the time under ketamine.

Discussion

This study establishes a robust anesthetized baboon model for BOLD fMRI studies of visual and somatosensory–motor stimulations on a 3 T human scanner. Under our experimental conditions, paralysis was necessary to achieve reproducible activations. Adequate anesthesia was determined by carefully titrating dosages without paralytic based on physiological parameters. At the appropriate dosages, both isoflurane (0.8–1.0%) and ketamine (6–8 mg/kg/h) in the presence of vecuronium paralytic (0.2 mg/kg followed by 10% every 45–90 min) yield reliable BOLD fMRI responses and comparable sensitivity. Robust activations are detected in the S1, S2, V, M, SMA, as well as subcortical structures—the LGN and Th. This baboon fMRI model sets the stage for high-resolution functional mapping of normal brain functions and dysfunctions in disease states.

Brain size and spatial resolution

The smaller brain volume of baboon compared to human makes it necessary to acquire images with higher spatial resolution in order to achieve comparable parcellation of functional structures (Stelkis and Erwin, 1988; Stephan et al., 1981). A 1.5 × 1.5 × 4 mm voxel herein in the baboon brain corresponds to a 4 × 4 × 5.5 mm voxel in the human brain accounting for volumetric differences. This spatial resolution is slightly worse than the typical spatial resolution used in human brain mapping fMRI studies to date.

Spatial resolution can be improved by either reducing FOV or increasing the matrix size, both requiring stronger gradients to prevent unacceptably long readout time for EPI acquisition. Gradient strengths on human scanners (typically 40–60 mT/m, compared to 400–1500 mT/m on small-animal MRI systems) could be a limiting factor. Head-only gradient inserts capable of 80–100 mT/m are becoming commercially available, which would benefit NHP fMRI studies (Kolster et al., 2009). Signal-to-noise ratio (SNR) decreases with increasing spatial resolution. SNR can be increased by high field scanners and/or using RF coils made to fit specifically for NHP heads. RF coils of different sizes to fit various NHP head sizes may not be readily available on clinical scanners. The present study utilized the commercially available 12-channel human head coil and a 3 T clinical scanner to facilitate clinical translation of future protocol development. Future studies could include custom-made RF coils and head-only gradient insert to improve SNR and/or spatial resolution.

BOLD percent changes

In this study, robust BOLD fMRI responses were detected in baboon under 0.8–1.0% isoflurane or 6–8 mg/kg/h ketamine with paralysis. BOLD percent changes under isoflurane and ketamine anesthesia were overall similar, ranging from 0.48 to 1.07%. Our findings are consistent with the 0.5–1.0% BOLD signal changes of somatosensory stimulations reported in anesthetized macaques at 1.5 T (Disbrow et al., 1999; Hayashi et al., 1999). Another fMRI study on

macaques used a custom-designed vertical bore 4.7 T Bruker scanner and a combination of very low anesthetic dose of isoflurane (0.3–0.5%) and opiates (fentanyl and morphine) along with mivacurium paralytic (Logothetis, 2002; Logothetis et al., 2001). In that study, BOLD responses to reversing checkerboard were 4.2 ± 2.5% in the striate cortex and 2.6 ± 1.5% in the LGN (Logothetis et al., 1999). These percent changes are significantly higher than those reported herein, which could be due to lower isoflurane dosage (0.3–0.5% versus 0.8– 1.0%), "stronger" visual stimulus (i.e., reversing checkerboard versus flickers), higher field strength (4.7 T versus 3 T), and/or reduced partial volume effect due to higher spatial resolution.

The low temporal resolution of 2.5 s precluded the detection of early negative changes, which have been a controversial issue in the literature (Duong et al., 2000a; Grinvald et al., 2000; Kim et al., 2000; Yacoub et al., 2001). We did not detect significant post-stimulus undershoot which have been observed in many, but not all, awake human and anesthetized animals studies. Post-stimulus undershoot has been found to be dependent on the nature of the stimulus and anesthetics. The BOLD signal sources of the post-stimulus undershoot remain controversial and have been discussed elsewhere (Buxton et al., 2004; Chen and Pike, 2009; Lu et al., 2004).

Isoflurane versus ketamine

Both anesthetics yielded similar BOLD sensitivity as indicated by similar Z scores. Although not statistically different between the two anesthetics, the overall BOLD percent changes were slightly higher under ketamine than isoflurane (0.75% versus 0.58% averaging across all structures). A possible explanation is that isoflurane is a strong vasodilator (Matta et al., 1999). Basal cerebral blood flow (CBF) under 1% or 2% isoflurane has been shown to be higher than that under awake conditions in the same animals (Sicard et al., 2003). Our preliminary data on baboons showed that CBF was slightly higher under 1% isoflurane than 6–8 mg/kg/h ketamine in the same animals (data not shown). If vessels under basal conditions are already significantly dilated, stimulus-evoked dilation could be less effective, resulting in smaller CBF, and thus BOLD, increase. Another possible explanation is that isoflurane suppresses neuronal responses more than ketamine. A study comparing the effects of several anesthesia on rats using 2-[18F]-fluoro-2-deoxy-D-glucose (FDG) PET (Matsumura et al., 2003) found that ketamine (150 mg/kg as initial dose followed by 50 mg/kg every 30 min, i.m.) only reduced the whole-brain FDG uptake slightly, not statistically different from conscious rats. On the other hand, the whole-brain FDG uptake in rats anesthetized with isoflurane (1.5%) was significantly lower than conscious rats. The isoflurane:ketamine FDG uptake ratio was only 0.64.

Activation frequencies

S1, S2, M and V activations were detected essentially in all trials and all studies. LGN activations were detected 64% of the time under isoflurane and 70% under ketamine. SMA and Th activations were detected 36% and 45% of the time under isoflurane, respectively, and 60% of the time under ketamine. As expected, activations in the subcortical structures were detected less frequently under both anesthetics compared to those in the primary cortices. Moreover, subcortical activations were less frequently detected under isoflurane than ketamine, suggesting isoflurane suppresses higher brain functions more severely, consistent with a FDG study (Matsumura et al., 2003). Percent changes of subcortical nuclei when activated, however, were not weaker than those of the primary sensory cortices.

Thalamic activation is expected during both visual and sensory tasks. However, reports of subcortical BOLD fMRI activations in anesthetized animal models are sparse. In rat forepaw stimulation studies, subcortical fMRI responses were almost never detected (Duong et al., 2000b; Keilholz et al., 2004; Lee et al., 2002; Liu et al., 2004; Mandeville et al., 1998; Silva

et al., 2000) except under noxious stimulations (Shih et al., 2009; Zhao et al., 2008). Similarly, in anesthetized macaques, S2 and subcortical activations were not detected in somatosensory stimulation studies (Hayashi et al., 1999). The differences between ours and Hayashi's study could be due to the anesthetic protocol and the nature of stimuli.

Activation patterns

Visual stimulation at 10 Hz flicker rate activated both visual cortices and LGN. V1 and V2 are widely reported in many functional imaging studies in anesthetized animal models. LGN activations in anesthetized animals, although they are less frequently reported in the literature, have been observed in anesthetized macaques at 3 T (Wibral et al., 2007) and 4.7 T (Logothetis et al., 1999) and in anesthetized cat at 9.4 T (Zhang et al., 2008), among others.

Vibrotactile stimuli herein activated S1, S2, M, SMA and Th. While S1 has been reported in anesthetized macaque monkeys (Disbrow et al., 1999, 2000; Hayashi et al., 1999), we are pleasantly surprised by the S2, M, and SMA activations as well as the strong thalamic activations detected in anesthetized baboons in this study. Bilateral S2 activations are more often reported than M, SMA, and Th in human studies (Golaszewski et al., 2002a,b; Graham et al., 2001; Li Hegner et al., 2007; Ruben et al., 2001). Moreover, cortical evoked potential studies on macaques suggest that neurons in S2 have receptive field from both contralateral and ipsilateral of the body side (Whitsel et al., 1969). In passive stimulations paradigms, M and SMA are not generally expected. However, early studies with vibrotactile stimulation in human have shown M and SMA, which has been suggested to be associated with tonic vibration reflex via activation of the cutaneous muscle spindles of the palm (Golaszewski et al., 2002a,b).

Every sensory system except the olfactory system is routed through the thalamic nuclei to relay information from the periphery to the cerebral cortex. Thalamic activations of vibrotactile stimuli have only been reported in a few awake human studies (Chakravarty et al., 2009a, b; Li Hegner et al., 2007) but are not generally detected in anesthetized animal models. For example, a PET study in awake humans showed that passive finger movement activated only the contralateral S1 and S2, whereas active finger movement activated the contralateral M, SMA, bilateral S2, and premotor cortex, in addition to the contralateral S1 (Mima et al., 1999). Thalamic activation was not detected. Another PET study in awake humans showed that passive bilateral vibrotactile stimulation activated bilateral S1 and SMA(Fox et al., 1987) but again no thalamic activation was detected. Similarly, many BOLD fMRI studies of vibrotactile stimulations in awake humans showed contralateral S1 and S2 activations, and some showed bilateral S2, contralateral M, and SMA activations, but only a few showed bilateral Th activations (Golaszewski et al., 2002a,b;Graham et al., 2001; Li Hegner et al., 2007). The pattern of activations reported by Li Hegner et al. in awake humans is similar to that observed in the current study in anesthetized baboons. The robust BOLD responses in the Th could also be associated with the tonic vibration reflex and/or direct thalamocortical projections. This anesthetized baboon model using vibrotactile stimulation offers a unique means to study Th function using non-invasive BOLD fMRI.

Conclusions

This study establishes a robust baboon model for BOLD fMRI studies on a 3 T clinical MRI scanner. Under our experimental conditions, paralysis is necessary to achieve reproducible activations in both cortical and subcortical structures. Both isoflurane and ketamine at the appropriate doses are suitable for fMRI studies and yield comparable sensitivity. A major contribution of the current study is that this anesthetized baboon model provides a means to activate thalamic and other subcortical responses, opening up a new avenue for fMRI studies of the these subcortical structures in large NHPs. Future study will focus on improving spatial

resolution and utilizing this fMRI protocol to map functional changes associated with stroke and epilepsy. This baboon fMRI model has the potential to facilitate future applications of large NHPs in neuroscience research, including comparative functional brain mapping across species.

Acknowledgments

The authors thank Dr. Peter Kochunov for providing the baboon brain template and John Roby for technical supports. This study was supported by AHA EIA grant 0940104N, NIH R01 NS045879, a CTSA imaging supplement (parent grant: UL1RR025767) to TQD, and NIH R21 grant NS 065431 to CAS.

References

Andersen AH, Zhang Z, Barber T, Rayens WS, Zhang J, Grondin R, Hardy P, Gerhardt GA, Gash DM. Functional MRI studies in awake rhesus monkeys: methodological and analytical strategies. J. Neurosci. Methods 2002;118:141–152. [PubMed: 12204305]

Bianciardi M, Cerasa A, Patria F, Hagberg GE. Evaluation of mixed effects in event-related fMRI studies: impact of first-level design and filtering. NeuroImage 2004;22:1351–1370. [PubMed: 15219607]

Buxton RB, Uludağ K, Dubowitz DJ, Liu TT. Modeling the hemodynamic response to brain activation. NeuroImage 2004;23 Suppl 1:S220–S233. [PubMed: 15501093]

Chakravarty MM, Broadbent S, Rosa-Neto P, Lambert CM, Collins DL. Design, construction, and validation of an MRI-compatible vibrotactile stimulator intended for clinical use. J. Neurosci. Methods 2009a;184:129–135. [PubMed: 19631690]

Chakravarty MM, Rosa-Neto P, Broadbent S, Evans AC, Collins DL. Robust S1, S2, and thalamic activations in individual subjects with vibrotactile stimulation at 1.5 and 3.0 T. Hum. Brain Mapp 2009b;30:1328–1337.

Chen JJ, Pike GB. Origins of the BOLD post-stimulus undershoot. NeuroImage 2009;46:559–568. [PubMed: 19303450]

Chen LM, Turner GH, Friedman RM, Zhang N, Gore JC, Roe AW, Avison MJ. High-resolution maps of real and illusory tactile activation in primary somatosensory cortex in individual monkeys with functional magnetic resonance imaging and optical imaging. J. Neurosci 2007;27:9181–9191. [PubMed: 17715354]

Del Zoppo GJ, Copeland BR, Harker LA, Waltz TA, Zyroff J, Hanson SR, Battenberg E. Experimental acute thrombotic stroke in baboons. Stroke 1986;17:1254–1265. [PubMed: 3810730]

Disbrow E, Roberts TP, Slutsky D, Krubitzer L. The use of fMRI for determining the topographic organization of cortical fields in human and nonhuman primates. Brain Res 1999;829:167–173. [PubMed: 10350543]

Disbrow EA, Slutsky DA, Roberts TP, Krubitzer LA. Functional MRI at 1.5 tesla: a comparison of the blood oxygenation level-dependent signal and electrophysiology. Proc. Natl. Acad. Sci. U. S. A 2000;97:9718–9723. [PubMed: 10931954]

Dubowitz DJ, Bernheim KA, Chen DY, Bradley WG Jr, Andersen RA. Enhancing fMRI contrast in awake-behaving primates using intravascular magnetite dextran nanopartieles. Neuroreport 2001a; 12:2335–2340. [PubMed: 11496106]

Dubowitz DJ, Chen DY, Atkinson DJ, Scadeng M, Martinez A, Andersen MB, Andersen RA, Bradley WG Jr. Direct comparison of visual cortex activation in human and non-human primates using functional magnetic resonance imaging. J. Neurosci. Methods 2001b;30:71–80.

Duong TQ. Diffusion tensor and perfusion MRI of non-human primates. Methods 2010;50:125–135. [PubMed: 19665567]

Duong TQ, Kim DS, Uğurbil K, Kim SG. Spatiotemporal dynamics of the BOLD fMRI signals: toward mapping submillimeter cortical columns using the early negative response. Magn. Reson. Med 2000a; 44:231–242. [PubMed: 10918322]

Duong TQ, Silva AC, Lee SP, Kim SG. Functional MRI of calcium-dependent synaptic activity: cross correlation with CBF and BOLD measurements. Magn. Reson. Med 2000b;43:383–392. [PubMed: 10725881]

Ferris CF, Snowdon CT, King JA, Duong TQ, Ziegler TE, Ugurbil K, Ludwig R, Schultz-Darken NJ, Wu Z, Olson DP, Sullivan JM Jr, Tannenbaum PL, Vaughan JT. Functional imaging of brain activity in conscious monkeys responding to sexually arousing cues. Neuroreport 2001;12:2231–2236. [PubMed: 11447340]

Ferris CF, Snowdon CT, King JA, Sullivan JM Jr, Ziegler TE, Olson DP, Schultz-Darken NJ, Tannenbaum PL, Ludwig R, Wu Z, Einspanier A, Vaughan JT, Duong TQ. Activation of neural pathways associated with sexual arousal in non-human primates. J. Magn. Reson. Imaging 2004;19:168–175. [PubMed: 14745749]

Fisher RS. Animal models of the epilepsies. Brain Res. Rev 1989;14:245–278. [PubMed: 2679941]

Fisher M. Recommendations for standards regarding preclinical neuroprotective and restorative drug development. Stroke 1999;30:2752–2758. [PubMed: 10583007]

Fox PT, Burton H, Raichle ME. Mapping human somatosensory cortex with positron emission tomography. J. Neurosurg 1987;67:34–43. [PubMed: 3298565]

Fukuda S, del Zoppo G. Models of focal cerebral ischemia in the nonhuman primate. Ilar J 2003;44:96–104. [PubMed: 12652004]

Gamlin PD, Ward MK, Bolding MS, Grossmann JK, Twieg DB. Developing functional magnetic resonance imaging techniques for alert macaque monkeys. Methods 2006;38:210–220. [PubMed: 16481198]

Golaszewski SM, Siedentopf CM, Baldauf E, Koppelstaetter F, Eisner W, Unterrainer J, Guendisch GM, Mottaghy FM, Felber SR. Functional magnetic resonance imaging of the human sensorimotor cortex using a novel vibrotactile stimulator. NeuroImage 2002a;17:421–430. [PubMed: 12482095]

Golaszewski SM, Zschiegner F, Siedentopf CM, Unterrainer J, Sweeney RA, Eisner W, Lechner-Steinleitner S, Mottaghy FM, Felber S. A new pneumatic vibrator for functional magnetic resonance imaging of the human sensorimotor cortex. Neurosci. Lett 2002b;324:125–128. [PubMed: 11988343]

Graham SJ, Staines WR, Nelson A, Plewes DB, McIlroy WE. New devices to deliver somatosensory stimuli during functional MRI. Magn. Reson. Med 2001;46:436–442. [PubMed: 11550233]

Greer PJ, Villemagne VL, Ruszkiewicz J, Graves AK, Meltzer CC, Mathis CA, Price JC. MR atlas of the baboon brain for functional neuroimaging. Brain Res. Bull 2002;58:429–438. [PubMed: 12183022]

Grinvald A, Slovin H, Vanzetta I. Non-invasive visualization of cortical columns by fMRI. Nat. Neurosci 2000;3:105–107. [PubMed: 10649563]

Hayashi T, Konishi S, Hasegawa I, Miyashita Y. Mapping of somatosensory cortices with functional magnetic resonance imaging in anaesthetized macaque monkeys. Eur. J. Neurosci 1999;11:4451–4456. [PubMed: 10594672]

Jones NL, Robertson DG, Kane JW. Difference between end-tidal and arterial PCO2 in exercise. J. Appl. Physiol 1979;47:954–960. [PubMed: 511720]

Keilholz SD, Silva AC, Raman M, Merkle H, Koretsky AP. Functional MRI of the rodent somatosensory pathway using multislice echo planar imaging. Magn. Reson. Med 2004;52:89–99. [PubMed: 15236371]

Kennedy RC, Shearer MH, Hildebrand W. Nonhuman primate models to evaluate vaccine safety and immunogenicity. Vaccine 1997;15:903–908. [PubMed: 9234544]

Killam EK. Photomyoclonic seizures in the baboon, Papio papio. Fed. Proc 1979;38:2429–2433. [PubMed: 39008]

Kim D-S, Duong TQ, Kim S-G. High-resolution mapping of iso-orientation columns by fMRI. Nat. Neurosci 2000;3:164–169. [PubMed: 10649572]

King JA, Garelick TS, Brevard ME, Chen W, Messenger TL, Duong TQ, Ferris CF. Procedure for minimizing stress for fMRI studies in conscious rats. J. Neurosci. Methods 2005;148:154–160. [PubMed: 15964078]

Kochunov P, Davis MD. Development of structural MR brain imaging protocols to study genetics and maturation. Methods 2009;50:136–146. [PubMed: 19665566]

Kolster H, Mandeville JB, Arsenault JT, Ekstrom LB, Wald LL, Vanduffel W. Visual field map clusters in macaque extrastriate visual cortex. J. Neurosci 2009;29:7031–7039. [PubMed: 19474330]

Lee S-P, Silva AC, Kim S-G. Comparison of diffusion-weighted high-resolution CBF and spin-echo BOLD fMRI at 9.4 T. Magn. Reson. Med 2002;47:736–741. [PubMed: 11948735]

Leigh SR. Brain growth, life history, and cognition in primate and human evolution. Am. J. Primatol 2004;62:139–164. [PubMed: 15027089]

Li Hegner Y, Saur R, Veit R, Butts R, Leiberg S, Grodd W, Braun C. BOLD adaptation in vibrotactile stimulation: neuronal networks involved in frequency discrimination. J. Neurophysiol 2007;97:264–271. [PubMed: 17065253]

Liu ZM, Schmidt KF, Sicard KM, Duong TQ. Imaging oxygen consumption in forepaw somatosensory stimulation in rats under isoflurane anesthesia. Magn. Reson. Med 2004;52:277–285. [PubMed: 15282809]

Locher CP, Witt SA, Herndier BG, Tenner-Racz K, Racz P, Levy JA. Baboons as an animal model for human immunodeficiency virus pathogenesis and vaccine development. Immunol. Rev 2001;183:127–140. [PubMed: 11782253]

Logothetis NK. The neural basis of the blood-oxygen-level-dependent functional magnetic resonance imaging signal. Philos. Trans. R. Soc. Lond. B Biol. Sci 2002;357:1003–1037. [PubMed: 12217171]

Logothetis NK, Guggenberger H, Peled S, Pauls J. Functional imaging of the monkey brain. Nat. Neurosci 1999;2:555–562. [PubMed: 10448221]

Logothetis NK, Pauls J, Augath M, Trinath T, Oeltermann A. Neurophysiological investigation of the basis of the fMRI signal. Nature 2001;412:150–157. [PubMed: 11449264]

Lu H, Golay X, Pekar JJ, Van Zijl PC. Sustained poststimulus elevation in cerebral oxygen utilization after vascular recovery. J. Cereb. Blood Flow Metab 2004;24:764–770. [PubMed: 15241184]

Mandeville JB, Marota JJ, Kosofsky BE, Keltner JR, Weissleder R, Rosen BR. Dynamic functional imaging of relative cerebral blood volume during rat forepaw stimulation. Magn. Reson. Med 1998;39:615–624. [PubMed: 9543424]

Matsumura A, Mizokawa S, Tanaka M, Wada Y, Nozaki S, Nakamura F, Shiomi S, Ochi H, Watanabe Y. Assessment of microPET performance in analyzing the rat brain under different types of anesthesia: comparison between quantitative data obtained with microPET and ex vivo autoradiography. NeuroImage 2003;20:2040–2050. [PubMed: 14683708]

Matta BF, Heath KJ, Tipping K, Summors AC. Direct cerebral vasodilatory effects of sevoflurane and isoflurane. Anesthesiology 1999;91:677–680. [PubMed: 10485778]

Mima T, Sadato N, Yazawa S, Hanakawa T, Fukuyama H, Yonekura Y, Shibasaki H. Brain structures related to active and passive finger movements in man. Brain 1999;122:1989–1997. [PubMed: 10506099]

Pinsk MA, DeSimone K, Moore T, Gross CG, Kastner S. Representations of faces and body parts in macaque temporal cortex: a functional MRI study. Proc. Natl. Acad. Sci. U. S. A 2005;102:6996–7001. [PubMed: 15860578]

Rogers J, Hixson JE. Baboons as an animal model for genetic studies of common human disease. Am. J. Hum. Genet 1997;61:489–493. [PubMed: 9326312]

Ruben J, Schwiemann J, Deuchert M, Meyer R, Krause T, Curio G, Villringer K, Kurth R, Villringer A. Somatotopic organization of human secondary somatosensory cortex. Cereb. Cortex 2001;11:463–473. [PubMed: 11313298]

Shih Y-YI, Chen C-CV, Shyu B-C, Lin Z-J, Chiang Y-C, Jaw F-S, Chen Y-Y, Chang C. A new scenario for negative functional magnetic resonance imaging signals: endogenous neurotransmission. J. Neurosci 2009;29:3036–3044. [PubMed: 19279240]

Sicard K, Shen Q, Brevard ME, Sullivan R, Ferris CF, King JA, Duong TQ. Regional cerebral blood flow and BOLD responses in conscious and anesthetized rats under basal and hypercapnic conditions: implications for functional MRI studies. J. Cereb. Blood Flow Metab 2003;23:472–481. [PubMed: 12679724]

Silva AC, Lee SP, Iadecola C, Kim SG. Early temporal characteristics of cerebral blood flow and deoxyhemoglobin changes during somatosensory stimulation. J. Cereb. Blood Flow Metab 2000;20:201–206. [PubMed: 10616809]

Smith SM, Jenkinson M, Woolrich MW, Beckmann CF, Behrens TEJ, Johansen-Berg H, Bannister PR, De Luca M, Drobnjak I, Flitney DE, Niazy RK, Saunders J, Vickers J, Zhang Y, De Stefano N, Brady JM, Matthews PM. Advances in functional and structural MR image analysis and implementation as FSL. NeuroImage 2004;23 Suppl 1:S208–S219. [PubMed: 15501092]

Smith SM, Beckmann CF, Ramnani N, Woolrich MW, Bannister PR, Jenkinson M, Matthews PM, McGonigle DJ. Variability in fMRI: a re-examination of inter-session differences. Hum. Brain Mapp 2005;24:248–257. [PubMed: 15654698]

Stefanacci L, Reber P, Costanza J, Wong E, Buxton R, Zola S, Squire L, Albright T. fMRI of monkey visual cortex. Neuron 1998;20:1051–1057. [PubMed: 9655492]

Stelkis, H.; Erwin, J. Comparative Primate Biology. New York: Alan R. Liss; 1988. Comparative size of brains and brain components.

Stephan H, Frahm H, Baron G. New and revised data on volumes of brain structures in insectivores and primates. Folia Primatol. (Basel) 1981;35:1–29. [PubMed: 7014398]

Szabó CA, Narayana S, Kochunov PV, Franklin C, Knape K, Davis MD, Fox PT, Leland MM, Williams JT. PET imaging in the photosensitive baboon: case-controlled study. Epilepsia 2007;48:245–253. [PubMed: 17295617]

Takano Y, Sakamoto O, Kiyofuji C, Ito K. A comparison of the end-tidal CO2 measured by portable capnometer and the arterial PCO2 in spontaneously breathing patients. Respir. Med 2003;97:476–481. [PubMed: 12735663]

Vanduffel W, Fize D, Mandeville JB, Nelissen K, Van Hecke P, Rosen BR, Tootell RB, Orban GA. Visual motion processing investigated using contrast agent-enhanced fMRI in awake behaving monkeys. Neuron 2001;32:565–577. [PubMed: 11719199]

Whitsel BL, Petrucelli LM, Werner G. Symmetry and connectivity in the map of the body surface in somatosensory area II of primates. J. Neurophysiol 1969;32:170–183. [PubMed: 4975532]

Wibral M, Muckli L, Melnikovic K, Scheller B, Alink A, Singer W, Munk MH. Time-dependent effects of hyperoxia on the BOLD fMRI signal in primate visual cortex and LGN. NeuroImage 2007;35:1044–1063. [PubMed: 17321759]

Woolrich MW, Jbabdi S, Patenaude B, Chappell M, Makni S, Behrens T, Beckmann C, Jenkinson M, Smith SM. Bayesian analysis of neuroimaging data in FSL. NeuroImage 2009;45:S173–S186. [PubMed: 19059349]

Yacoub E, Shmuel A, Pfeuffer J, Van De Moortele PF, Adriany G, Ugurbil K, Hu X. Investigation of the initial dip in fMRI at 7 Tesla. NMR Biomed 2001;14:408–412. [PubMed: 11746933]

Zhang N, Zhu X-H, Zhang Y, Chen W. An fMRI study of neural interaction in large-scale cortico-thalamic visual network. NeuroImage 2008;42:1110–1117. [PubMed: 18598771]

Zhao F, Zhao T, Zhou L, Wu Q, Hu X. BOLD study of stimulation-induced neural activity and resting-state connectivity in medetomidine-sedated rat. NeuroImage 2008;39:248–260. [PubMed: 17904868]

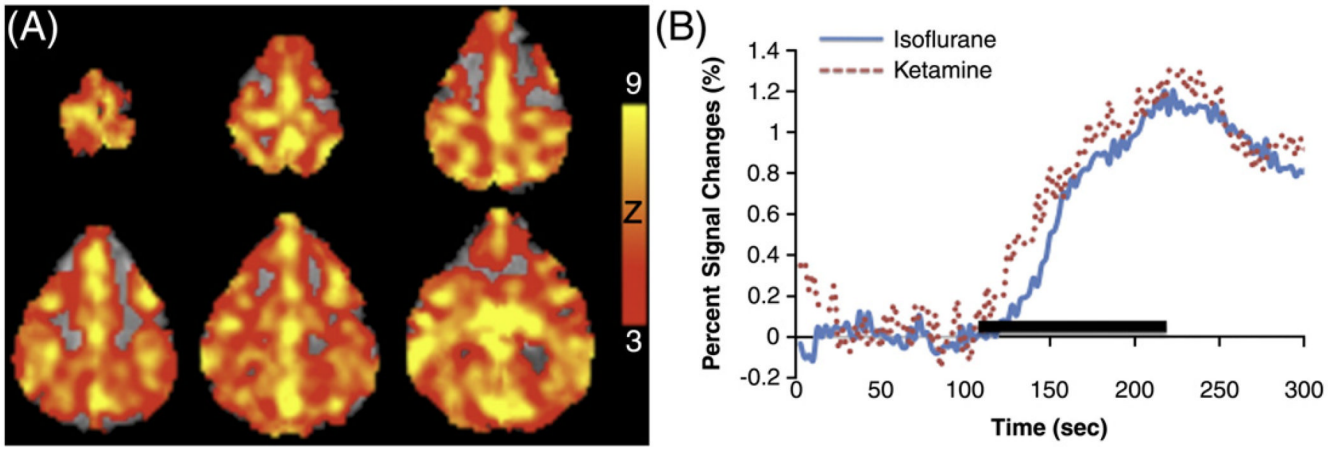

Fig. 1.

(A) BOLD fMRI "activation" maps under isoflurane and (B) averaged time courses of hypercapnic (5% CO_2) inhalation under isoflurane (blue line) and ketamine (red dash line). Paralytic was used for both anesthetics. Color bar indicates Z scores.

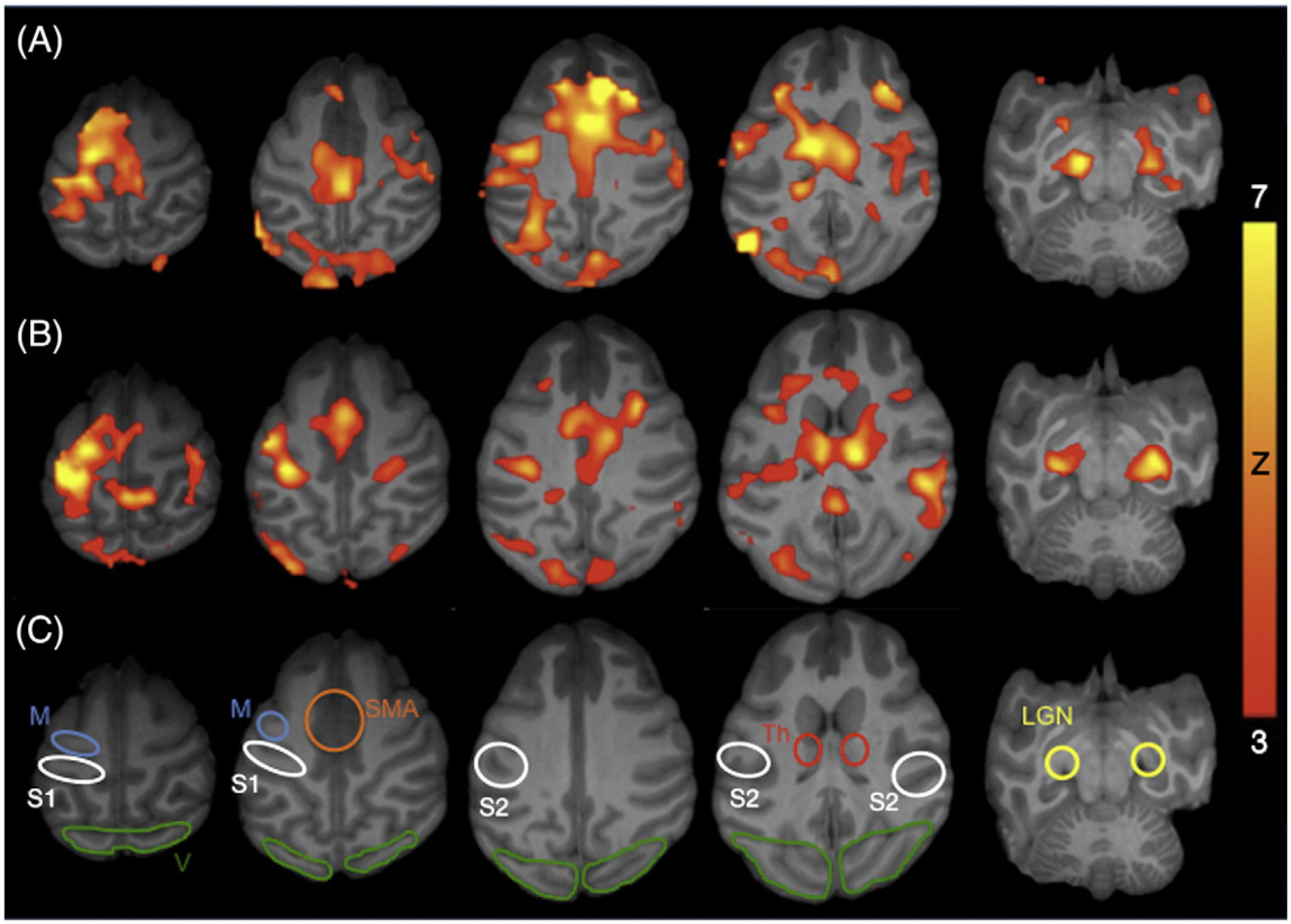

Fig. 2.

BOLD fMRI activation maps responding to simultaneous visual and somatosensory–motor stimulation from a representative subject under (A) isoflurane and (B) ketamine. Paralytic was used for both anesthetics. Color bar indicates Z scores. (C) Regions of interests (ROIs) used in subsequent quantitative analysis include the primary (S1) and secondary (S2) somatosensory cortex, primary motor cortex (M), supplementary motor area (SMA), thalamus (Th), visual cortex (V), and lateral geniculate nuclei (LGN).

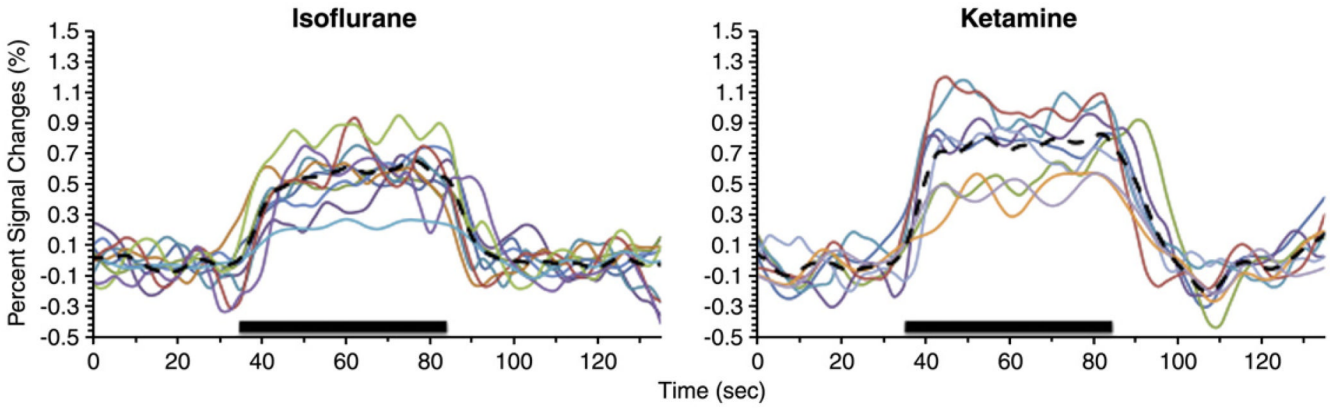

Fig. 3.

Individual time courses of all stimulation trials from the S1 under isoflurane and ketamine. Thick dash lines indicate the means of all traces. ROI used is shown in Fig. 2C.

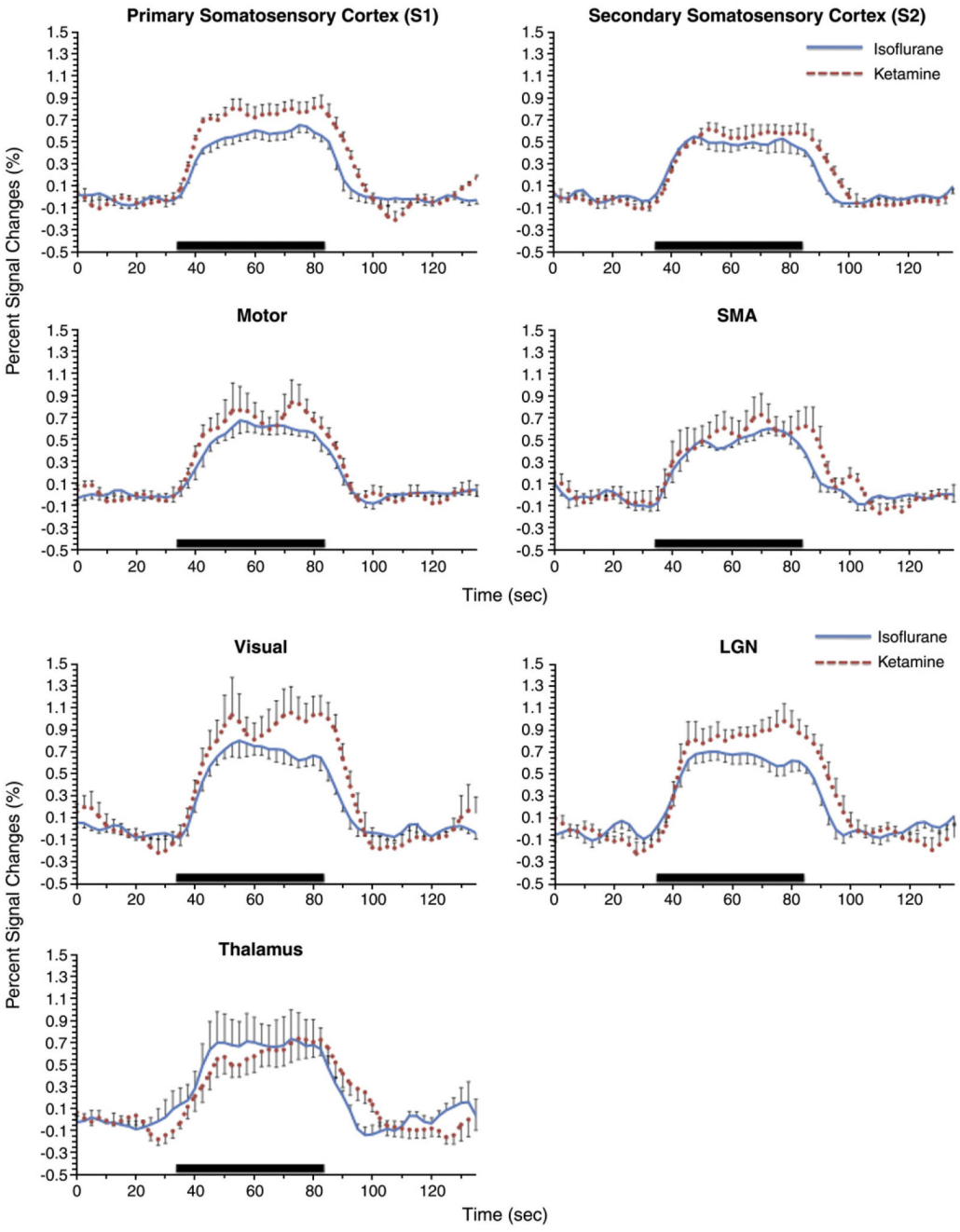

Fig. 4.

Averaged BOLD fMRI time courses from ROIs shown in Fig. 2C under isoflurane (blue line) and ketamine (red dotted line). Paralytic was used for both anesthetics. Error bars indicate the standard errors of the means for 11 trials under isoflurane and 10 trials under ketamine.

Table 1

Detection incidence, BOLD percent changes and Z scores from ROIs (mean±SEM, 11 trials for isoflurane (Iso), and 10 trials for ketamine (Ket)).

	Detection incidence		BOLD % changes		Z scores	
	Iso	Ket	Iso	Ket	Iso	Ket
S1	100%	100%	0.55±0.05	0.69±0.08	4.7±0.4	4.7±0.4
S2	82%	100%	0.48±0.06	0.53±0.08	4.0±0.3	4.6±0.3
M	91%	70%	0.56±0.05	0.66±0.12	4.6±0.3	4.2±0.3
SMA	36%	60%	0.50±0.05	0.74±0.13	4.8±0.4	4.3±0.3
Th	45%	60%	0.65±0.23	0.71±0.13	4.6±0.4	4.3±0.4
V	100%	90%	0.67±0.07	0.85±0.16	4.2±0.2	4.2±0.3
LGN	64%	70%	0.68±0.07	1.07±0.19	4.9±0.4	5.5±0.6